

## Ab Initio/DFT and AIM Studies on Dual Hydrogen-Bonded Complexes of 2-Hydroxypyridine/2-Pyridone Tautomerism

Dong-ling Wu, Lang Liu, Guang-fei Liu, and Dian-zeng Jia\*

Institute of Applied Chemistry, Xinjiang University, Urumqi 830046, People's Republic of China

Received: January 11, 2007; In Final Form: March 26, 2007

The second-order Møller-Plesset (MP2) and density functional theory (DFT) calculations have been carried out to investigate the structures and stabilities of hydrogen (H-) bonded 2-hydroxypyridine (2HP)/2-pyridone (2PY) dimeric forms as well as 2HP–2PY complexes. The results on single-point counterpoise (CP) correction of these complexes were compared against CP-optimized correction. The nature of the intermolecular contacts in the sense of normal H-bond or blue-shifting H-bond was determined on the basis of harmonic vibrational, atom-in-molecule (AIM), and natural bond orbital (NBO) analysis. A blue-shifting C–H···N H-bond was found and NBO analysis revealed a slight decrease in the population of the contacting  $\sigma_{\text{C-H}}^*$  antibonding orbital as the primary reason of the C–H contraction. Good correlations have been established between the interaction energies and the H-bond distances versus other characteristic H-bond parameters.

### 1. Introduction

Studies on hydrogen (H-) bonded systems, in particular those involving new types of H-bonds (such as “dihydrogen bond”,<sup>1,2</sup> “bifurcated H-bond”,<sup>3</sup> and “blue-shifting H-bond”),<sup>4,5</sup> have come to light in recent years. Accurate techniques should be applied to study the blue-shifting H-bonds, because reliable estimation of the frequency shift is crucial to differentiate between red- and blue-shift values. The problem concerns the structural evaluation and particularly the influence of the basis set superposition error (BSSE). This error occurs because different basis sets are used for evaluation of the energies of the supersystem and its subsystems. The supersystem, having a larger basis set than the subsystems, undergoes an artificial stabilization. Although other approaches to correct the BSSE have been proposed in the literature,<sup>6–10</sup> the counterpoise (CP) correction proposed by Boys and Bernardi<sup>11</sup> seems to be the practically applicable approach for eliminating the BSSE. Usually, one adds CP correction as a single-point correction to the previously optimized geometry of the complex (the expression “single-point CP correction” will be used to mean this treatment), which means that the structure of the complex is optimized not on the CP corrected potential energy surface (PES) but on the standard PES. Since the final stabilization energy, the structure, and other properties (e.g., vibration frequencies) of a complex are affected by the CP correction, one should use CP to correct the optimized geometry (expressed as “CP-optimized correction”) as well as the interaction energy.<sup>4,12</sup> Early in the 1990s, there was evidence<sup>12,13</sup> that the interaction energy, geometry, and vibrational frequency on the CP corrected PES differed from the corresponding values on the uncorrected surface (more traditional, single-point CP correction). Several examples<sup>13,14</sup> of molecular orbital calculations where CP was included in the optimization had been performed. Simon et al.<sup>12</sup> offered a straightforward method for optimizing geometry on the CP corrected PES and demonstrated that various properties obtained from CP-optimized and traditional ways differed significantly. Similar results for other H-bonded systems were obtained by Hobza and Havlas.<sup>15</sup>

Besides IR and NMR spectra, crystal structure information often provides strong experimental evidence for detecting H-bonds as well as for describing their strength. On the other hand, on the basis of natural bond orbital (NBO) analysis, Hobza and Havlas<sup>4</sup> revealed that the origin of X–H bond strength changed in the classical H-bond and blue-shifting H-bond. For the classical H-bond, the electron density (ED) is transferred from lone electron pairs of the proton acceptor (Y) to the antibonding orbital of the proton donor ( $\sigma_{\text{X-H}}^*$ ). The increase of ED in  $\sigma_{\text{X-H}}^*$  weakens the X–H bond, which leads to its elongation and concomitant lowering of the X–H stretch frequency. However, the blue-shifting H-bond represents a more complicated “two-step” process, which involves ED transferred to remote parts of the proton donor, resulting in geometrical change that leads to a X–H contraction and a blue shift. Further, the atom-in-molecule (AIM) theory<sup>16</sup> is often applied to study the properties of a variety of H-bonded systems. Koch and Popelier<sup>17</sup> proposed a set of criteria for the existence of H-bond on the basis of the AIM theory. It has been proved that these criteria are valid for standard and nonconventional H-bonds and that they provide a basis to distinguish these interactions from van der Waals interactions. To differentiate between H-bond and blue-shifting H-bond, Cubero et al.<sup>18</sup> suggested that it was necessary to supplement those criteria with information on the changes in the electron density of the X–H bond upon complexation. Many studies<sup>19</sup> have demonstrated the correlations between the interaction energies and the intermolecular distances, and so forth, versus topological parameters such as the electron density  $\rho(r)$  at bond critical point (BCP). To the best of our knowledge, these correlations have been well documented in the single H-bonded complexes. However, studies on the multiple H-bonded complexes, especially those involving different types of H-bonds, are scarce.<sup>17,20</sup> Early in 1995, Koch and Popelier<sup>17</sup> established an excellent correlation between the interaction energies and the total  $\rho(r)$  values ( $E_{\text{IMPT}} = -995.62\rho_b + 1.5919$ ,  $R = 0.998$ , where  $\rho_b$  refers to the sum of  $\rho(r)$  when more than one intermolecular BCP is present). Furthermore, we have established good linear correlations between the interaction energies  $De$  and the sum of the H-bond distances ( $\ln(-De) = 8.09 - 1.38\Sigma R_{\text{H}\cdots\text{Y}}$ ,  $R = 0.972$ ) as well

\* To whom correspondence should be addressed. Tel.: +86-991-8580032. Fax: +86-991-8581006. E-mail: jdz@xju.edu.cn.

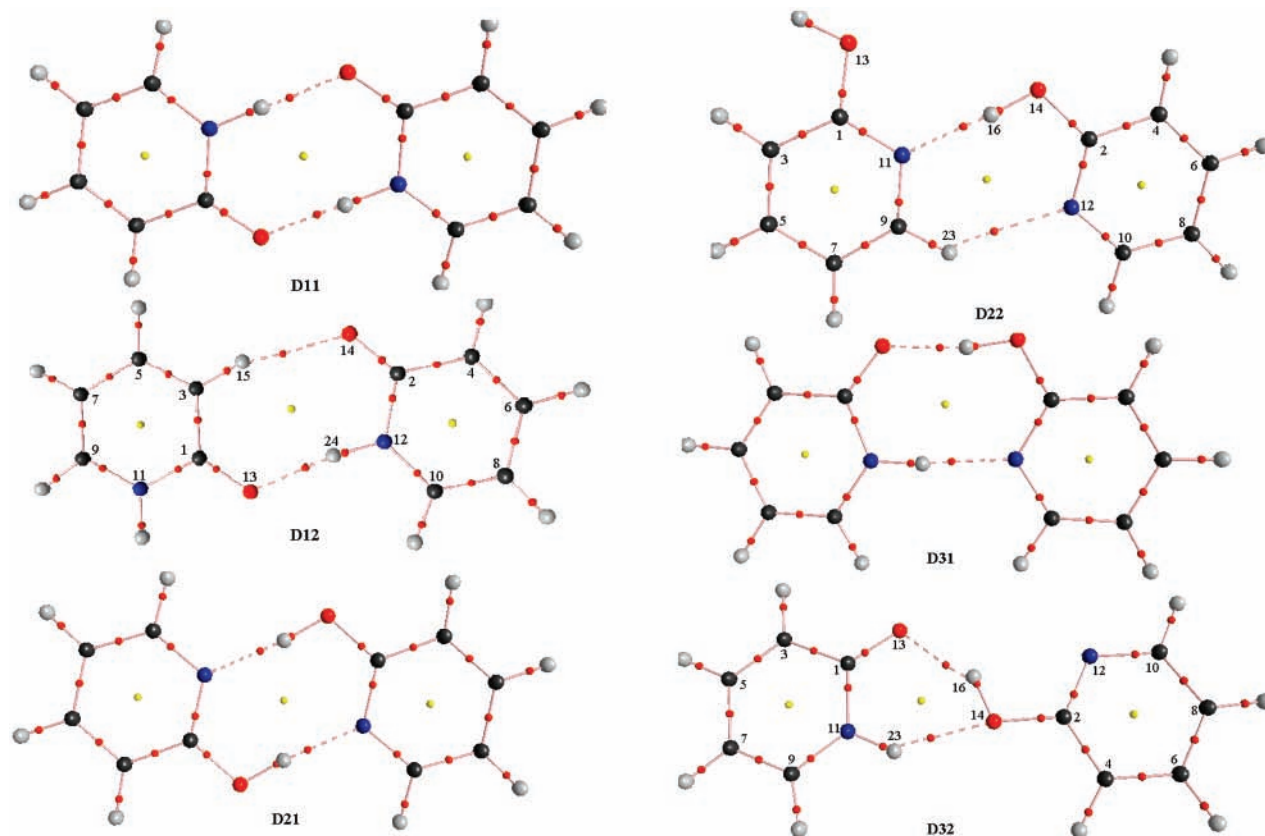


**Figure 1.** Molecular graphs of complexes. Large circles correspond to attractors attributed to atomic positions: gray, H; blue, N; black, C; red, O. Small circles are attributed to critical points: red, bond critical point; yellow, ring critical point. The left part is unit 1 and the right part is unit 2. H-bonds are represented as dotted lines.

as the sum of  $\rho(r)$  ( $\ln(-De) = 0.40 + 35.47 \sum \rho_{H...Y}$ ,  $R = 0.958$ ) and its Laplacian  $\nabla^2\rho(r)$  at intermolecular BCPs ( $\ln(-De) = 0.39 + 10.11 \sum \nabla^2\rho_{H...Y}$ ,  $R = 0.949$ ) for the four 2,4-dithiothymine–water complexes (the values of  $De$ ,  $R_{H...Y}$ ,  $\rho_{H...Y}$ , and its Laplacian derived from He et al.)<sup>21</sup> These findings impel us to find such correlations, particularly in those cases involving different types of H-bonds.

For the 2-hydroxypyridine (2HP)/2-pyridone (2PY) system, previous studies focused on the tautomerism of the isomers and possible complexes<sup>22</sup> because of their relevance to proton transfer and nucleic acid chemistry. Several studies on clusters of 2HP/2PY, in particular those with water<sup>23</sup> and ammonia,<sup>24</sup> have been reported in the literature. Matsuda et al.<sup>25</sup> found that the “ring-type” or “linear-type” H-bonded structures were appropriate for 2PY and its H-bonded clusters. Some groups<sup>26–30</sup> investigated the homodimer of 2PY ( $D_{11}$ ) and 2HP ( $D_{21}$ ) and the heterodimers of 2PY with 2HP ( $D_{31}$ ), as all of them formed cyclic H-bonds and were more or less planar. (Their structures are presented in Figure 1.) Müller et al.<sup>27</sup> experimentally investigated the intermolecular vibrations of the supersonically cooled  $D_{11}$  and  $D_{31}$ . Chou and Wei<sup>28</sup> had performed extensive ab initio calculations to  $D_{11}$ ,  $D_{21}$ , and  $D_{31}$  in the gas phase and in solution. They showed that the formation of the conjugated dual H-bond would induce charge redistribution, resulting in additional stabilization energy. Alkorta and Elguero<sup>29</sup> performed density functional theory (DFT) calculation to the same complexes, and amino-substituted 2-aminopyridines and exponential relationships were found between  $\rho(r)$  and its  $\nabla^2\rho(r)$  at intermolecular BCP versus H-bond distance for 2-aminopyridines. However, it appears that AIM theory has not been used to characterize the H-bonded interactions of complexes of 2HP/2PY, which are of interest here.

In addition to the complex known with certainty, we have further optimized three 2HP/2PY complexes in this paper (Figure 1). The main aim is to compare the interaction energies and other properties of these complexes evaluated by the single-point CP correction and the CP-optimized correction. The other goal is to investigate the nature of H-bonds and to attempt to find the correlations of all cases.

## 2. Computational Details

On the basis of the investigation of structures, intermolecular vibrational frequencies, and interaction energies of  $D_{11}$ , Müller et al.<sup>30</sup> showed that second-order Møller-Plesset (MP2) with 6-31+G\*\* and 6-311++G\*\* basis sets predicted that the H-bond distances were in good agreement with experiment. B3LYP was the most effective method to predict the intermolecular vibrations. Thus, in this work, all the geometries were optimized at B3LYP and MP2 levels using 6-31+G\*\* and 6-311++G\*\* basis sets. The minimum nature of monomers and complexes was confirmed by frequency calculation only using DFT method considering computational cost.

The BSSE has been evaluated using the counterpoise (CP) method proposed by Boys and Bernardi.<sup>11</sup> The uncorrected ( $De$ ) and corrected ( $De^{BSSE}$ ) interaction energies can be evaluated using eqs 1–3.

$$De = E_{AB}^{ab}(AB) - E_A^a(A) - E_B^b(B) \quad (1)$$

$$BSSE = [E_A^a(AB) - E_A^{ab}(AB)] + [E_B^b(AB) - E_B^{ab}(AB)] \quad (2)$$

$$De^{BSSE} = De + BSSE \quad (3)$$

**TABLE 1: Relative Energy  $E_{\text{rel}}$ , Interaction Energy  $D_e$  (kcal/mol), and Geometrical Parameters of the H-Bonds of the Six Complexes at B3LYP/6-31++G\*\* Level**

	D <sub>11</sub> N—H···O	D <sub>12</sub> N—H···O/C—H···O	D <sub>21</sub> O—H···N	D <sub>22</sub> O—H···N/C—H···N	D <sub>31</sub> N—H···N/O—H···O	D <sub>32</sub> N—H···O/O—H···O
$E_{\text{rel}}$	0.000 <sup>a</sup> 0.711 <sup>b</sup> 0.707 <sup>c</sup>	8.576 9.104 9.100	4.761 5.721 5.715	17.835 18.516 18.510	4.777 5.586 5.583	11.580 12.102 12.099
$D_e$	-19.994 <sup>a</sup> -19.284 <sup>b</sup> -19.288 <sup>c</sup>	-11.418 -10.890 -10.899	-16.163 -15.203 -15.215	-3.087 -2.407 -2.419	-15.682 -14.873 -14.877	-8.879 -8.286 -8.292
$R_{\text{X}\cdots\text{Y}}$ (Å)	2.767 <sup>a,b</sup> 2.775 <sup>c</sup>	2.852/3.277 2.864/3.293	2.708 2.720	2.812/3.355 2.826/3.370	2.905/2.627 2.909/2.632	2.927/2.674 2.935/2.684
$R_{\text{H}\cdots\text{Y}}$ (Å)	1.724 <sup>a,b</sup> 1.731 <sup>c</sup>	1.826/2.216 1.839/2.232	1.698 1.711	1.817/2.507 1.832/2.523	1.866/1.628 1.870/1.632	2.073/1.781 2.081/1.792
$\Delta R_{\text{X-H}}$ (mÅ)	30.32 <sup>a,b</sup> 29.85 <sup>c</sup>	18.90/3.90 18.20/3.83	42.26 40.98	25.67/-0.4 24.70/-0.41	29.09/35.47 29.05/35.57	5.43/23.76 5.33/23.17
$\nu_{\text{X-H}}$ (cm <sup>-1</sup> )	3088 <sup>a,b</sup> 3093 <sup>c</sup>	3265/3176 3274/3179	2958 <sup>asym</sup> 2979	3240/3192 3258/3193	3096 <sup>asym</sup> (3018 <sup>sym</sup> ) 3095 (3017)	3518/3322 3520/3331
$\Delta\nu_{\text{X-H}}$ (cm <sup>-1</sup> )	-516 <sup>a,b</sup> -511 <sup>c</sup>	-339/-54 -330/-51	-813 -792	-531/13 -513/14	-508 <sup>asym</sup> / -675 <sup>asym</sup> -509 <sup>asym</sup> / -676 <sup>asym</sup>	-86/-449 -84/-440

<sup>a</sup> Uncorrected parameters. <sup>b</sup> Single-point CP corrected parameters. <sup>c</sup> CP-optimized corrected parameters.

where the subscripts A, B, and AB denote the molecular systems, the superscripts a, b, and ab denote the monomer- and dimer-centered basis sets, and the notations in round brackets denote that they are calculated at the optimized geometry of the (sub)system A, B, and AB, respectively. For example,  $E_{\text{A}}^{\text{ab}}$  (AB) is the energy of A at the equilibrium of AB, calculated in the dimer-centered basis set.

To obtain deeper insight into the nature of H-bonded interactions, AIM analysis was performed using AIM2000.<sup>31</sup> The BCPs of the X—H bonds as well as the H···Y interactions were found, and their features were analyzed. Further, analysis of the charge distribution and charge-transfer processes were performed using NBO partitioning scheme.<sup>32</sup> All calculations were performed with GAUSSIAN03 program.<sup>33</sup>

### 3. Results and Discussion

#### 3.1. Structures, Binding Energy, and Vibrational Analysis.

Experimental data on the relative stability of the 2HP and 2PY tautomeric forms provide a basis to validate the computational method used. It has been found that DFT methods predict incorrectly that in the gas phase 2PY is more stable than 2HP. Only methods including high electron correlation effects are able to reproduce the experimental findings.<sup>27,29</sup> The DFT energetic results indicate that 2PY is more stable than 2HP by 0.47 kcal/mol, even at B3LYP/6-311++G\*\* (by about 0.87 kcal/mol and 0.79 kcal/mol including vibrational-zero-point energy (ZPE), respectively). It is different from the results derived from Müller et al.,<sup>27b</sup> where they found that B3LYP/6-311++G\*\* total energy calculations (including ZPE) predicted 2HP molecule to be 0.79 kcal/mol more stable than 2PY. Similar to the work reported earlier,<sup>27</sup> MP2 method is able to reproduce the experimental findings.

The normal complexes of 2HP/2PY (Figure 1: D<sub>11</sub>, D<sub>21</sub>, D<sub>31</sub>) have been widely studied both experimentally<sup>27</sup> and computationally,<sup>28–30</sup> which have yielded precise H-bond distances and vibrational frequencies as well as interaction energies. Tables 1 and 2 give the B3LYP and MP2 values of H-bond distances and interaction energies, which are consistent with the corresponding values reported previously. Focusing on D<sub>11</sub> values, two equivalent N—H···O H-bonds are calculated at B3LYP/6-311++G\*\* to be  $R(\text{N}\cdots\text{O}) = 2.78$  Å and the interaction energy to be  $D_e = -19.49/-18.78$  kcal/mol, while the corre-

sponding MP2 values are  $R(\text{N}\cdots\text{O}) = 2.74$  Å and  $D_e = -22.08/-18.33$  kcal/mol, respectively. By comparison, the calculated  $R(\text{N}\cdots\text{O})$  is 2.77 Å<sup>27b</sup> or 2.78 Å<sup>30</sup> with B3LYP method and 2.74 Å with MP2 method. The calculated  $D_e$  is -19.50/-18.78 kcal/mol<sup>29</sup> and -19.12/-18.45 kcal/mol<sup>27b</sup> with B3LYP method and -22.48/-18.36 kcal/mol<sup>30</sup> with MP2 method. Compared with MP2 results, B3LYP's H-bond distance is longer but turns out to be in agreement with experimental value (measured value is 2.77 Å).<sup>34</sup>

The relative energy of D<sub>21</sub> calculated at B3LYP with respect to D<sub>11</sub> is 5.305 kcal/mol. However, the results at MP2/6-311++G\*\* predict that D<sub>21</sub> is the most stable form. The discrepancy may arise from the fact that in the gas phase 2HP is more stable than 2PY with MP2 method, while DFT method predicts a reverse stability order of the two tautomeric forms.

Compared with MP2 values, except for D<sub>21</sub>, H-bond distances at B3LYP are longer by 0.01–0.05 Å, and MP2 calculation gives larger uncorrected  $D_e$  (-5 to -22 kcal/mol) which is in line with shorter H-bond distance. For all B3LYP calculations, the values of BSSE are small (0.5–0.9 kcal/mol), corresponding to only 3–6% of the uncorrected  $D_e$ . The MP2 method gives relatively larger BSSE than that of B3LYP. Thus, it is no surprise that CP corrected  $D_e^{\text{BSSE}}$  values with B3LYP are close to the ones with MP2 method.

Normally, the complex is optimized using standard supermolecular gradient optimization and, only at the end, the CP correction is added (e.g., single-point CP correction). In principle, since BSSE causes the intermolecular interactions to be artificially too attractive, CP correction should make the complexes less stable with consequent longer intermolecular distances and lower H-bond stretch frequencies than the normally optimized geometry. In this part, we report the interaction energies, geometries, and vibrational frequencies of the complexes obtained from CP-optimized way, which have been summarized in Table 1. It is obvious that the CP-optimized geometry is of lower energy than that of single-point CP correction. As expected, the H-bond distances are always longer calculated by CP-optimized way. The largest change (0.016 Å) occurs for C<sub>9</sub>—H<sub>23</sub>···N<sub>12</sub> H-bond of D<sub>22</sub>. As further expected, the interactions of all cases become more attractive. However, it is indicated that CP-optimized way does not influence  $D_e$  substantially because the differences are rather small. Thus, the

**TABLE 2: Calculated Energy and Geometrical and Topological Parameters (the Single-Point-Corrected De's Are in Parenthesis) for the Six Complexes at B3LYP/6-311++G\*\* and MP2/6-311++G\*\***

	D11 N-H...O	D12 N-H...O/C-H...O	D21 O-H...N	D22 O-H...N/C-H...N	D31 N-H...N/O-H...O	D32 N-H...O/O-H...O
$E_{rel}$	0.000 <sup>a</sup> 0.000 <sup>b</sup>	8.305 8.417	5.305 -1.223	18.195 11.038	5.014 1.648	11.715 8.887
De	-19.486 <sup>a</sup> (-18.780) -22.083 <sup>b</sup> (-18.328)	-11.181 (-10.678) -13.667 (-11.048)	-15.930 (-15.036) -17.660 (-14.182)	-3.040 (-2.382) -5.399 (-2.905)	-15.347 (-14.558) -17.612 (-14.104)	-8.646 (-8.127) -10.373 (-7.974)
$R_{X...Y}$ (Å)	2.780 <sup>a</sup> 2.740 <sup>b</sup>	2.858/3.293 2.822/3.264	2.727 2.734	2.821/3.357 2.813/3.303	2.911/2.643 2.870/2.645	2.921/2.684 2.885/2.680
$R_{H...Y}$ (Å)	1.740 <sup>a</sup> 1.696 <sup>b</sup>	1.833/2.237 1.797/2.203	1.723 1.738	1.829/2.511 1.825/2.478	1.875/1.648 1.832/1.657	2.064/1.805 2.024/1.798
$\Delta^c R_{X-H}$ (mÅ)	28.43 <sup>a</sup> 30.15 <sup>b</sup>	18.22/3.74 17.57/3.04	39.02 32.19	24.99/-0.32 22.09/-0.53	28.59/32.86 27.86/28.92	5.74/22.38 5.17/20.77
$\Delta\nu_{X-H}$ (cm <sup>-1</sup> )	-475 <sup>a</sup>	-323/-50	-748	-509/12	-459 <sup>asym</sup> / -641 <sup>asym</sup> -540 <sup>sym</sup> / -722 <sup>sym</sup>	-90/-414
$\rho_{H...Y}/10^{-3}$ (au)	28.49 <sup>a</sup> 29.81 <sup>b</sup>	24.27/13.05 25.11/13.70	31.92 29.71	26.50/10.59 25.60/11.41	26.07/31.67 27.25/29.57	15.78/25.66 16.72/25.16
$\nabla^2\rho_{H...Y}$ (au)	0.20 <sup>a</sup> 0.23 <sup>b</sup>	0.16/0.06 0.17/0.06	0.23 0.23	0.17/0.01 0.18/0.04	0.16/0.25 0.18/0.25	0.08/0.17 0.09/0.17
$\rho_{X-H}$ (au)	0.32 <sup>a</sup> 0.32 <sup>b</sup>	0.33/0.29 0.33/0.29	0.31 0.32	0.33/0.29 0.33/0.30	0.32/0.32 0.32/0.32	0.34/0.33 0.34/0.34
$\nabla^2\rho_{X-H}$ (au)	-1.65 <sup>a</sup> -1.92 <sup>b</sup>	-1.70/-0.99 -1.95/-1.05	-2.33 -2.51	-2.44/-1.01 -2.60/-1.11	-1.62/-2.40 -1.89/-2.56	-1.73/-2.46 -1.95/-2.61
$\Delta\rho_{X-H}/10^{-3}$ (au)	-21.62 <sup>a</sup> -25.23 <sup>b</sup>	-12.38/5.14 -12.89/4.08	-46.34 -42.04	-29.66/4.10 -29.60/3.56	-23.63/-39.79 -24.76/-38.50	-0.71/-26.54 -0.61/-27.46

<sup>a</sup> B3LYP/6-311++G\*\*, <sup>b</sup> MP2/6-311++G\*\*, <sup>c</sup>  $\Delta$  refers to change in indicated quantity as a result of formation of the complex.

following De is only calculated by single-point CP correction. Moreover, the X-H stretches except for that of D<sub>31</sub> are shifted to higher frequencies, which is largely because of the mixing of two intermolecular modes. The changes of lengths and harmonic stretch frequencies of X-H bonds upon complexation obtained from CP-optimized and single-point CP correction differ slightly.

Table 2 reports the changes of lengths and harmonic stretch frequencies of X-H bonds upon complexation. The C-H covalent bond length of C<sub>9</sub>-H<sub>23</sub>...N<sub>12</sub> is contracted by 0.32/0.53 mÅ upon complex D<sub>22</sub> formation, while the other X-H bonds are more or less elongated. The lengthening/shortening of X-H bonds upon complexation is also reflected in the change of the corresponding stretch frequencies. The larger red shift of X-H stretch frequencies is found in D<sub>11</sub>, D<sub>12</sub> (N<sub>12</sub>-H<sub>24</sub> 323 cm<sup>-1</sup>) and in D<sub>21</sub>, D<sub>22</sub> (O<sub>14</sub>-H<sub>16</sub> 509 cm<sup>-1</sup>) as well as in D<sub>31</sub>, D<sub>32</sub>. The C<sub>3</sub>-H<sub>15</sub> and N<sub>11</sub>-H<sub>23</sub> stretch frequencies also show red shifts upon the formation of D<sub>12</sub> and D<sub>32</sub> (50 cm<sup>-1</sup> and 90 cm<sup>-1</sup>, respectively). The considerably small values clearly support the existences of C<sub>3</sub>-H<sub>15</sub>...O<sub>14</sub> and N<sub>11</sub>-H<sub>23</sub>...O<sub>14</sub> H-bonds. Furthermore, the contraction of C-H bond and a blue shift of its stretch frequency (12 cm<sup>-1</sup>) found for the C<sub>9</sub>-H<sub>23</sub>...N<sub>12</sub> H-bond provides the basis for the concept of blue-shifting H-bond. More precise analysis of these H-bonds, especially the blue-shifting C-H...N H-bond, will be done below on the basis of AIM and NBO analysis.

**3.2. Topological Analysis.** AIM provides a means of mapping topological properties of the electron density to Lewis structure representations of molecules. The nature of bonding between atoms can be characterized by the value of  $\rho(r)$  and the sign of the Laplacian  $\nabla^2\rho(r)$  of the electron density at the bond critical point (BCP). Large  $\rho(r)$  values together with negative  $\nabla^2\rho(r)$  values represent shared interactions, characteristic of covalent bonds. In contrast, low  $\rho(r)$  values along with positive  $\nabla^2\rho(r)$

values are indicative of closed-shell interactions typically found in ionic bonds and H-bonds as well as in van der Waals interactions. Among those criteria to establish H-bond proposed by Koch and Popelier, "there is a BCP for the H...Y contact", "the value of  $\rho(r)$  at BCP of H...Y lies within the range of 0.002-0.040 au", and "the corresponding Laplacian is in the range from 0.024 to 0.139 au" seem to be the most important ones and the most frequently used.

Figure 1 presents the molecular graphs of the complexes considered in this study (i.e., D<sub>11</sub>, D<sub>12</sub>, D<sub>21</sub>, D<sub>22</sub>, D<sub>31</sub>, and D<sub>32</sub>). These graphs present the positions of attractors and of BCPs as well as bond paths connecting critical points. The configurations of the systems obtained at levels other than MP2/6-311++G\*\* were slightly different from those presented in Figure 1. Both B3LYP and MP2 methods predict planar minimum-energy structures. They are characterized by six- or eight-membered ring structures stabilized by two H-bond interactions. The formation of H-bond is reflected in the appearance of BCP linking the hydrogen atom to each O, N, or C atom. In addition, a common feature to all complexes is the occurrence of ring critical points, which are more or less placed in the middle of the planar structure. Analysis of  $\rho(r)$  shows two H-bond critical points for each complex, which are characterized by the values of  $\rho(r)$  in the range of 0.011-0.030 au and the positive values of  $\nabla^2\rho(r)$  varying from 0.040 to 0.249 au.

As far as Koch and Popelier's three criteria are concerned, analysis of the features at BCP of H...Y shows no relevant difference for the series of H-bonds. These criteria are focused on  $\rho(r)$  occurring between the H atom of the donor molecule and the acceptor atom. However, they do not suffice to distinguish between normal H-bonds and blue-shifting H-bonds, which are determined by subtle changes in  $\rho(r)$  of X-H bonds. The results in Table 3 show decreasing  $\rho(r)$  in the X-H bonds upon the formation of N-H...O, O-H...N, N-H...N, and

**TABLE 3: Results of NBO Analysis for the Changes in Indicated Quantity as a Result of the Complex Formation (MP2/6-311++g\*\*)**

	D <sub>11</sub> N-H...O	D <sub>12</sub> N-H...O/C-H...O	D <sub>21</sub> O-H...N	D <sub>22</sub> O-H...N/C-H...N	D <sub>31</sub> N-H...N/O-H...O	D <sub>32</sub> N-H...O/O-H...O
$\Delta q_X^a$	-0.103	-0.111/-0.059	-0.102	-0.097/0.101	-0.115/-0.089	-0.096/-0.138
$\Delta q_H$	0.075	0.065/0.047	0.055	0.057/0.027	0.070/0.060	0.040/0.064
$\Delta q_Y$	-0.188	-0.171/-0.149	-0.148	-0.093/-0.104	-0.150/-0.170	-0.138/-0.144
CT <sup>b</sup>	0.000	0.021	0.000	0.031	0.003	0.020
tot. EDT	0.00	42.24	0.00	61.01	6.15	39.96
$\Delta\sigma_{X-H}^* c$	+42.4	+26.11/+5.58	+50.53	+34.31/-0.34	+39.93/+44.25	+5.25/+26.30
$\Delta n_{1Y}$	-14.74	-10.20/-2.52	-34.6	-22.49/+1.44	-25.96/-15.39	-8.63/-8.65
$\Delta n_{2Y}$	-2.96	+1.80/+7.00		-5.74	-2.29/-1.96	
$\Delta\%s\text{-char}(X-H)$	3.04	2.67/1.62	6.02	5.41/1.21	3.13/5.58	1.25/4.09
$E^{(2)}n_{1Y} \rightarrow \sigma_{XH}^*$	9.28	6.95/1.97	35.65	23.76/1.42	28.02/9.30	4.50/5.35
$n_{2Y} \rightarrow \sigma_{XH}^*$	25.18	14.34/2.50			25.94	12.95
$R_{E(X-H)}^d$	38.94	23.35/11.77	952.25	$\infty/1.21$	43.53/60.16	17.39/ $\infty$

<sup>a</sup> The natural charge at individual atom. <sup>b</sup> Sum of the natural charges on the atoms of 2PY or 2HP of unit 1 of each complex. <sup>c</sup> Occupation of natural orbital:  $n_m$  refers to lone electron pair ( $m$  refers to LP number);  $\sigma^*$  refers to antibonding orbital. <sup>d</sup> Reference 48.

O-H...O H-bonds. However, the reverse effect occurs in C<sub>9</sub>-H<sub>23</sub>...N<sub>12</sub> H-bond of D<sub>22</sub>, which is exhibited by increase in  $\rho(r)$  of the C-H bond. It consists of the shortening of the C-H bond and a blue shift of its vibrational frequency. More interestingly, the C<sub>3</sub>-H<sub>15</sub>...O<sub>14</sub> H-bond in D<sub>12</sub>, which is characterized by the lengthening of the C-H bond and a red shift of its stretch frequency, also shows an increased  $\rho(r)$  in the C-H bond upon complexation. To differentiate between normal H-bond and blue-shifting H-bond, our results suggest that it is necessary to supplement information concerning the changes in the X-H bonds. However, the information does not suffice to distinguish between weak normal H-bond, such as C-H...O H-bond here, and blue-shifting H-bond.

**3.3. NBO Analysis.** The changes of the natural charges in the X, H, and Y atoms upon complexation and the net charge transfer (CT) from the proton acceptor monomer toward the proton donor monomer are compiled in Table 3. To become better electron donors, the proton acceptors Y gain charges in all complexes, while the H atoms become more polarized (lose charges in all cases), whereby promoting the proton donor-acceptor interaction. The natural charge at C<sub>9</sub> atom associated with C<sub>9</sub>-H<sub>23</sub>...N<sub>12</sub> H-bond is more positive and the C<sub>9</sub> atomic charge of D<sub>22</sub> is 0.17. On the contrary, the charges at other X atoms associated with X-H...Y H-bonds are more negative and the X atomic charges are negative even at C<sub>3</sub> (-0.34) in the C<sub>3</sub>-H<sub>15</sub>...O<sub>14</sub> H-bond of D<sub>12</sub>. It is known that the formation of a H-bonded complex involves charge transfer from the proton acceptor to the proton donor. The CT could not evaluate in structures of D<sub>11</sub> and D<sub>21</sub>, which is in line with the fact that D<sub>11</sub> and D<sub>21</sub> are linked by the equivalent antiparallel H-bonds. The trend of the total electron density transfer (EDT) of all cases is consistent with that of CT, namely, some amount of charge is transferred from unit 1 to unit 2. Similarly, the total electron density ED is also transferred from unit 1 to unit 2, where unit 1 acts as electron donor part. The results mean that as an electron donor, the O<sub>13</sub> atom associated with N<sub>12</sub>-H<sub>24</sub>...O<sub>13</sub> H-bond of D<sub>12</sub> is better than O<sub>14</sub> of O<sub>14</sub>...H<sub>15</sub>-C<sub>3</sub> H-bond, which is in line with the strength order of N<sub>12</sub>-H<sub>24</sub>...O<sub>13</sub> > O<sub>14</sub>...H<sub>15</sub>-C<sub>3</sub> obtained from the values of  $R_{H...Y}$  and  $\Delta\nu_{X-H}$ . The situation of other complexes is similar to that of D<sub>12</sub>. On the other hand, the direction means that the electron donor (O or N atom) in unit 1 is better than that of unit 2 with consequent stronger H-bond formation. The magnitude of CT or EDT seems to be strongly related to the difference between the two H...Y distances or the difference in strength between the two H-bonds in each complex. The correlations between them have been established ( $R = 0.920$  and  $0.914$ , respectively, Figure 2).

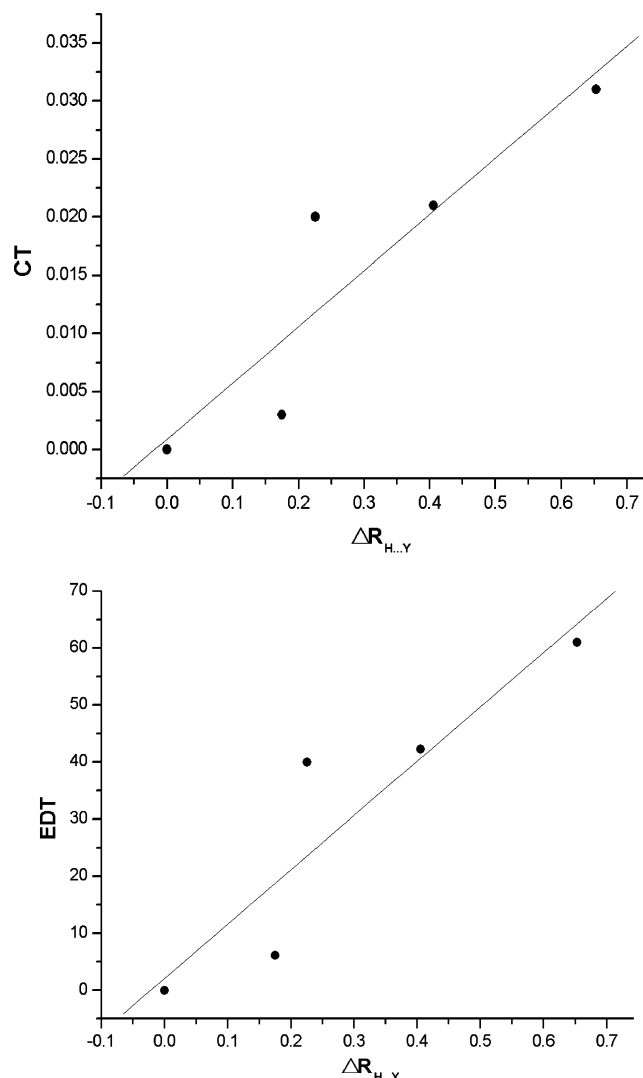


**Figure 2.** Correlations between the differences of the two H...Y distances of each complex and CT as well as EDT.

The complex formation alters the magnitude of ED between the lone electron pair ( $n$ ) and antibonding orbital ( $\sigma^*$ ) resulting in characteristic changes in the population of the interacting orbitals. These changes are strongly related to the changes in the respective bond distances upon complexation. Thus, more detailed information on CT process can be obtained by investigating the changes in the occupation of the acceptor and

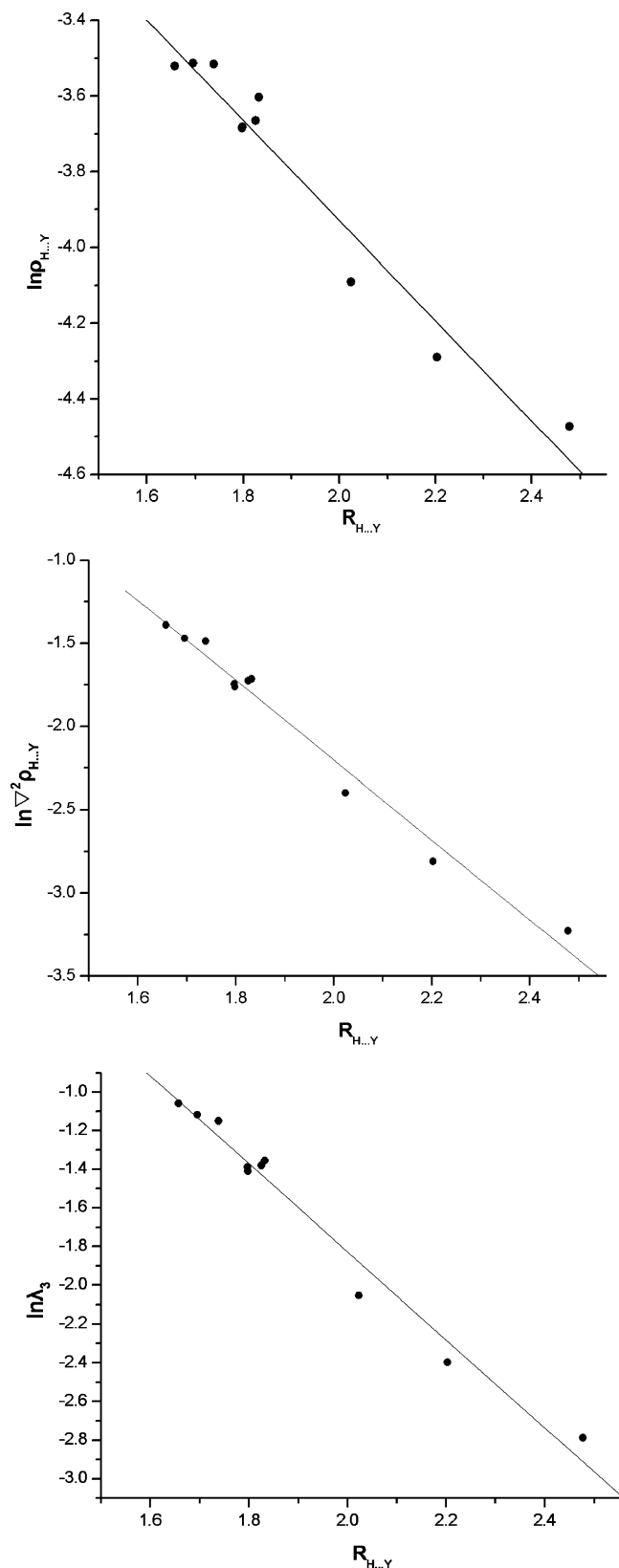


**Figure 3.** Correlations between  $R_{H...Y}$  and the logarithm of topological parameters at MP2 calculation.

donor orbitals and the second-order perturbation energies  $E^{(2)}$  corresponding to the inter- or intramolecular interactions. Investigating individual occupation in  $D_{11}$ , we found marked increases in the occupation of  $\sigma_{N-H}^*$  orbitals by 42.4 me while two strongest equally intermolecular interactions are found between  $n_O$  and  $\sigma_{N-H}^*$  orbital ( $E^{(2)} = 34.46$  kcal/mol). The

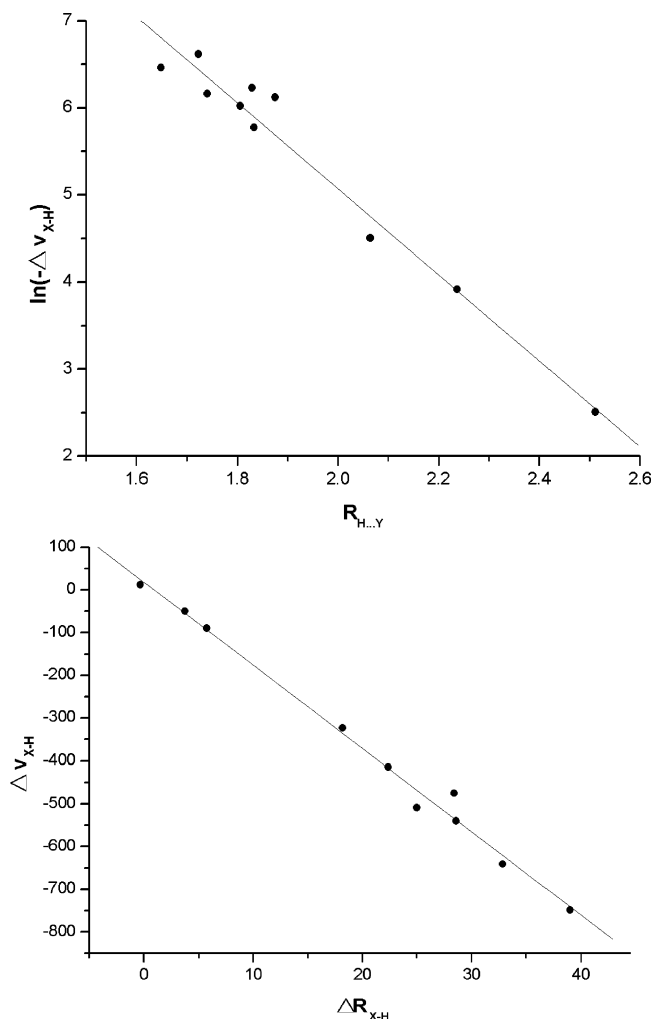


**Figure 4.** Correlations between the changes in X–H bond lengths as well as H-bond distances and the changes in vibrational stretch frequencies for the X–H bonds upon complexation.

increased occupation of  $\sigma_{N-H}^*$  orbitals leads to weakening of N–H bonds, their elongation, and concomitant red shift of stretch frequencies. The situation in  $D_{21}$  and  $D_{31}$  is similar to that of  $D_{11}$ . The occupation of  $\sigma_{N_{12}-H_{24}}^*$  and  $\sigma_{C_3-H_{15}}^*$  in  $D_{12}$  increased by 26.11 and 5.58 me, respectively. Two strongest intermolecular interactions are found between  $n_{O_{13}}$  and  $\sigma_{N_{12}-H_{24}}^*$  orbital ( $E^{(2)} = 21.29$  kcal/mol) and between  $n_{O_{14}}$  and  $\sigma_{C_3-H_{15}}^*$  orbital ( $E^{(2)} = 4.47$  kcal/mol). We also find the increased occupation of  $\sigma_{N_{11}-H_{23}}^*$  (5.25 me)/ $\sigma_{O_{14}-H_{16}}^*$  (26.30 me) in  $D_{32}$  and the corresponding  $E^{(2)}$  is 4.50 and 8.30 kcal/mol. Evidently, all the contacts mentioned above correspond to standard H-bonds of N–H $\cdots$ O, O–H $\cdots$ N, C–H $\cdots$ O, N–H $\cdots$ N, and O–H $\cdots$ O types.

As to  $D_{22}$ , the contact of  $O_{14}-H_{16}\cdots N_{11}$  is similar to that of the above-mentioned complexes. However, the situation of  $C_9-H_{23}\cdots N_{12}$  is obviously different. Our calculation predicts a small decrease of  $\sigma_{C_9-H_{23}}^*$  orbital occupation by 0.34 me and a weak increase of S-character of CH bond by 1.21%. Furthermore, the interaction between  $n_N$  and  $\sigma_{C_9-H_{23}}^*$  ( $E^{(2)} = 1.42$  kcal/mol) is small, while a stronger intramolecular interaction is found between  $n_{N_{11}}$  and  $\sigma_{C_9-H_{23}}^*$  ( $E^{(2)} = 4.62$  kcal/mol). The results reflect a different target of EDT in the  $C_9-H_{23}\cdots N_{12}$  contact, namely, ED is transferred from the proton acceptor  $N_{12}$  to the remote part (nonparticipating) of the proton donor. Let us recall that other X–H $\cdots$ Y interactions which are connected with increased occupation of  $\sigma_{X-H}^*$  also show increased

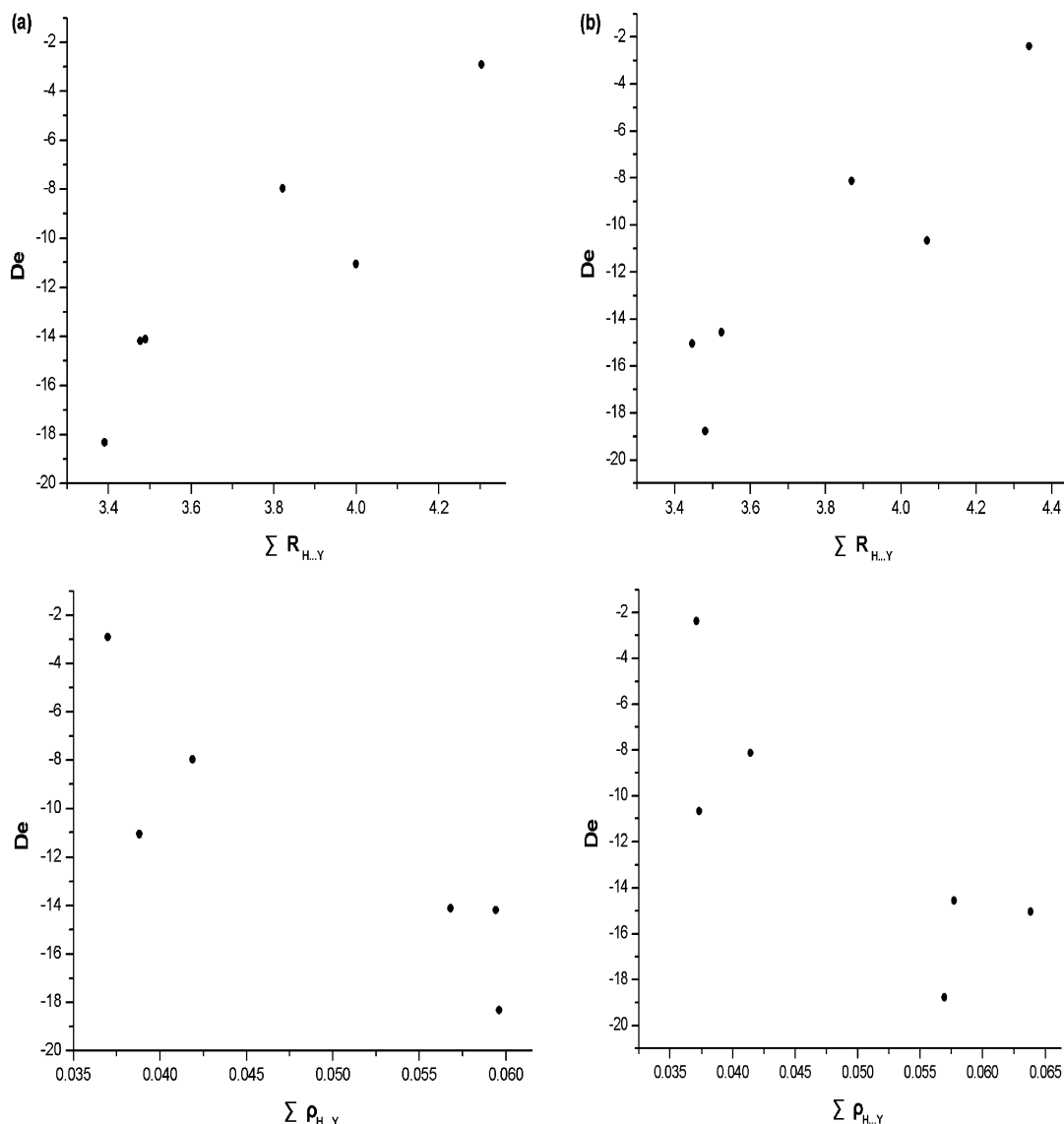


**Figure 5.** Correlation between  $\Sigma R_{H...Y}$  or  $\Sigma \rho_{H...Y}$  and the interaction energies  $D_e$ . (a) MP2 results; (b) B3LYP results.

S-characters of X–H bond. Hence, the occupation decreases of  $\sigma_{C9-H23}^*$  can be associated with the contraction of C–H bond which is the primary reason of formation of blue-shifting C–H $\cdots$ N H-bond. On the other hand, to study the cooperative effect between rehybridization and ED redistribution, Liu et al.<sup>35</sup> defined an index  $R_E$  as the ratio of the total increased  $E^{(2)}$  to the total decreased  $E^{(2)}$ . From  $R_E$  results of all interactions, as expected, for C<sub>9</sub>–H<sub>23</sub> $\cdots$ N<sub>12</sub> contact ( $R_E = 1.21$ ), ED redistribution effect overcomes the hyperconjugative effect, which leads to the ED in the  $\sigma_{C9-H19}^*$  orbital decrease. For other contacts ( $R_E > 10$ ), hyperconjugative domination leads to lengthening of X–H bonds and to red shifting of X–H stretch frequencies.

Several explanations have been proposed to rationalize the X–H contraction and blue shift of its stretch frequency. Alabugin et al.<sup>36</sup> have suggested that the observed structural reorganization of X–H bonds resulted from a balance of hyperconjugative bond weakening (increased occupation of XH  $\sigma^*$  antibonding orbital) and that rehybridization promoted bond strengthening (increased S-character of XH bond). Hobza and Havlas<sup>4</sup> showed that EDT from a lone pair of electron donors was directed to the remote part of electron acceptor. The X–H contraction is suggested to be the consequence of a subsequent structural reorganization in the remote moiety of the complex. Later, they<sup>37</sup> concluded that there were two ways to decrease

the X–H bond length and to obtain a blue shift of stretch frequency. The first, a direct way, is connected with a decrease of ED in the  $\sigma^*$  antibonding orbital; the second way is connected with the rehybridization of  $SP^N$  X–H hybrid orbital (an increase in the S-character of the hybrid bond). Our results are in good qualitative agreement with the statement.

**3.4. The Correlations Study.** The H-bond distance has always been used to estimate the strength of H-bond interaction. Many studies have demonstrated approximately linear relations between H-bond distances and interaction energies  $D_e$ . Through its implicit relationship with the topological properties of the electron density at the critical point, it permits the correlation of  $D_e$  to  $\rho(r)$  at the critical point. Thus, both H-bond distance and  $\rho(r)$  are related to the strength of H-bond interaction. Figure 3 shows the existence of a linear relationship between H-bond distance  $R_{H...Y}$  and the electron density  $\rho_{H...Y}$  and its Laplacian  $\nabla^2 \rho_{H...Y}$  as well as  $\lambda_3$  at the H $\cdots$ Y BCP, where  $\lambda_3$  is the positive eigenvalue of the Hessian of  $\rho(r)$ , which agrees with previous bond order–bond length relationship studies in H-bond complexes. Equations 4–9 show the linear relationships between them:

$$\text{MP2 results: } \ln \rho_{H...Y} = -1.08 - 1.32R_{H...Y}; \quad R = 0.976 \quad (4)$$

$$\ln \nabla^2 \rho_{\text{H}\cdots\text{Y}} = 2.59 - 2.40R_{\text{H}\cdots\text{Y}}; \quad R = 0.990 \quad (5)$$

$$\ln \lambda_3 = 2.72 - 2.27R_{\text{H}\cdots\text{Y}}; \quad R = 0.988 \quad (6)$$

$$\text{B}_3\text{LYP results: } \ln \rho_{\text{H}\cdots\text{Y}} = -1.08 - 1.42R_{\text{H}\cdots\text{Y}}; \\ R = 0.979 \quad (7)$$

$$\ln \nabla^2 \rho_{\text{H}\cdots\text{Y}} = 2.54 - 2.38R_{\text{H}\cdots\text{Y}}; \quad R = 0.992 \quad (8)$$

$$\ln \lambda_3 = 2.75 - 2.29R_{\text{H}\cdots\text{Y}}; \quad R = 0.990 \quad (9)$$

Furthermore, the complexation produces red or blue shifts in the X–H bond stretch that range between 12 and 750  $\text{cm}^{-1}$  depending on the system considered. In all cases, the smaller vibrational value is obtained for  $D_{m2}$  ( $m = 1, 2, 3$ ) complex followed by the corresponding  $D_{m1}$  one, in accordance with the relative strength of H-bond obtained. Good correlation between the change in the vibrational frequency of X–H bond and H-bond distance is established (Figure 4a:  $\ln(-\Delta\nu_{\text{X-H}}) = 14.95 - 4.94R_{\text{H}\cdots\text{Y}}$ ,  $R = 0.983$ ). The relationship between the changes in bond lengths and the changes in vibrational stretch frequencies of X–H bonds upon complexation in all cases is also established (Figure 4b:  $\Delta\nu_{\text{X-H}} = 18.34 - 19.45\Delta R_{\text{X-H}}$ ,  $R = 0.995$ ). It is noticeable that the C–H $\cdots$ O contact in  $D_{12}$  (here observed is  $R_{\text{H}\cdots\text{O}} > 2.2 \text{ \AA}$ , exhibited by the increase in  $\rho(r)$  of C–H bond), sometimes controversial in its consideration as normal H-bond and the C–H $\cdots$ N contact in  $D_{22}$  which is predicted to be blue-shifting H-bond, seems to follow the same phenomenological behavior as the other H-bonds within errors.

In terms of NBO theory, X–H $\cdots$ Y contact can be attributed to the localized  $n_{\text{Y}} \rightarrow \sigma_{\text{X-H}}^*$  interaction, that is, electronic delocalization from the filled lone pair of the electron donor Y into the unfilled antibonding of the electron acceptor X–H. The strengths of these interactions are estimated by second-order perturbation theory. Good linear correlation between the second-order perturbation energy  $E^{(2)}$  and H-bond distance (MP2 results:  $\ln E^{(2)} = 10.68 - 4.22R_{\text{H}\cdots\text{Y}}$ ,  $R = 0.968$ ; B3LYP results:  $\ln E^{(2)} = 9.82 - 3.80R_{\text{H}\cdots\text{Y}}$ ,  $R = 0.964$ ) as well as  $\rho(r)$  at H $\cdots$ Y BCP (MP2 results:  $\ln E^{(2)} = -23.16 + 1874.56\rho_{\text{H}\cdots\text{Y}}$ ,  $R = 0.971$ ; B3LYP results:  $\ln E^{(2)} = -16.51 + 1453.02\rho_{\text{H}\cdots\text{Y}}$ ,  $R = 0.975$ ) indicates that  $E^{(2)}$  as a result of the  $n_{\text{Y}} \rightarrow \sigma_{\text{X-H}}^*$  interaction reflects the attractive interaction in H-bond and can be used to characterize the strength of H-bond.

On the other hand, considering the dual contacted structures of all cases, we established the relationship between  $D_e$  and the total H-bond distance  $\Sigma R_{\text{H}\cdots\text{Y}}$  or the total electron density  $\Sigma \rho_{\text{H}\cdots\text{Y}}$  at H $\cdots$ Y BCP. The calculation results indicate that the total  $R_{\text{H}\cdots\text{Y}}$  and  $\rho_{\text{H}\cdots\text{Y}}$  provide an idea that the complexation strength seems to follow the same behavior as the usual complexes involving only one H-bond. Those with shorter  $\Sigma R_{\text{H}\cdots\text{Y}}$  or larger  $\Sigma \rho_{\text{H}\cdots\text{Y}}$  are the stronger ones. However, attempts to find correlations in all cases only yield poor values of  $R$  (Figure 5).

#### 4. Conclusion

Six dual H-bonded complexes of 2-HP/2-PY tautomerism are studied theoretically at both MP2 and DFT methods. The structural data of three normal complexes are close to that of early reports both experimentally and theoretically. The relative energies, interaction energies, and H-bond distances and their stretch frequencies obtained from single-point CP correction slightly differ from that of CP-optimized correction. Analysis

on the structural data and topological parameters shows that the normal H-bonds and blue-shifting C–H $\cdots$ N H-bond are formed upon complexation. As to the origin of the C–H contraction in the C–H $\cdots$ N H-bond, our NBO analysis reveals a slight decrease in the population of the  $\sigma_{\text{C-H}}^*$  orbital upon complexation. The correlation analysis shows that the parameters used for describing the H-bond strength are correlated and can be used to describe the properties of H-bonds.

**Acknowledgment.** This work was carried out with financial support from the National Natural Science Foundation of China (No.20462007) and the University Scientific Research Program of Education Bureau, Xinjiang Uygur Autonomous Region (XJEDU2004E01 and XJEDU2005S01).

#### References and Notes

- Richardson, T. B.; de Gala, S.; Crabtree, R. H.; Siegbahn, P. E. *M. J. Am. Chem. Soc.* **1995**, *117*, 12875.
- Alkorta, I.; Zborowski, K.; Elguero, J.; Solimannejad, M. *J. Phys. Chem. A* **2006**, *110*, 10279.
- Rybarczyk-Pirek, A. J.; Grabowski, S. J.; Nawrot-Modranka, J. *J. Phys. Chem.* **2003**, *107*, 9232.
- Hobza, P.; Havlas, Z. *Chem. Rev.* **2000**, *100*, 4253 and references therein.
- Barnes, A. J. *J. Mol. Struct.* **2004**, *704*, 3 and references therein.
- Jansen, H. B.; Ross, P. *Chem. Phys. Lett.* **1969**, *3*, 140.
- Mayer, I. *Int. J. Quantum Chem.* **1983**, *23*, 341.
- Almlöf, J.; Taylor, P. R. *J. Chem. Phys.* **1987**, *86*, 553.
- Sadlej, A. *J. Chem. Phys.* **1991**, *95*, 6705.
- Famulari, A.; Specchio, R.; Sironi, M.; Raimondi, M. *J. Chem. Phys.* **1998**, *108*, 3296.
- Boys, S. F.; Bernardi, F. *Mol. Phys.* **1970**, *19*, 553.
- Simon, S.; Duran, M.; Dannenberg, J. J. *J. Chem. Phys.* **1996**, *105*, 11024.
- Bouteiller, Y.; Behrouz, J. *Chem. Phys.* **1992**, *96*, 6033.
- Del Bene, J. E.; Mettee, H. D. *J. Phys. Chem.* **1991**, *95*, 5387.
- Hobza, P.; Havlas, Z. *Theor. Chem. Acc.* **1998**, *99*, 372.
- Bader, R. F. W. *Atoms in Molecules: A Quantum Theory*; Oxford University Press: New York, 1990.
- Koch, U.; Popelier, P. L. A. *J. Phys. Chem.* **1995**, *99*, 9747.
- Cubero, E.; Orozco, M.; Hobza, P.; Luque, F. J. *J. Phys. Chem.* **1999**, *103*, 6394.
- (a) Bader, R. F. W. *Chem. Rev.* **1991**, *91*, 893. (b) Alkorta, I.; Elguero, J. *J. Am. Chem. Soc.* **2002**, *124*, 1488. (c) Grabowski, S. J. *J. Phys. Chem. A* **2001**, *105*, 10739.
- Tian, S. X. *J. Phys. Chem. B* **2004**, *108*, 20388.
- He, W.; Xue, Y.; Zhang, H.; Tian, A.; Wong, N. B. *J. Phys. Chem. B* **2006**, *110*, 1416.
- (a) Scanlan, M. J.; Hillier, I. H.; MacDowell, A. A. *J. Am. Chem. Soc.* **1983**, *105*, 3568. (b) Field, M. J.; Hillier, I. H.; Guest, M. F. *J. Chem. Soc., Chem. Commun.* **1984**, 1310. (c) Wong, M. W.; Wiberg, K. B.; Frisch, M. J. *J. Am. Chem. Soc.* **1992**, *114*, 1645. (d) Sobolewski, A. L.; Adamowicz, L. *J. Phys. Chem.* **1996**, *100*, 3933. (e) Sato, H.; Hirata, F.; Sakaki, S. *J. Phys. Chem. A* **2004**, *108*, 2097. (f) Li, Q. S.; Fang, W. H.; Yu, J. G. *J. Phys. Chem. A* **2005**, *109*, 3983.
- (a) Held, A.; Pratt, D. W. *J. Am. Chem. Soc.* **1993**, *115*, 9708. (b) Florio, G. M.; Gruenloh, C. J.; Quimpo, R. C.; Zwier, T. S. *J. Chem. Phys.* **2000**, *113*, 11143. (c) Dkhissi, A.; Adamowicz, L.; Maes, G. *Chem. Phys. Lett.* **2000**, *324*, 127.
- (a) Dkhissi, A.; Adamowicz, L.; Maes, G. *J. Phys. Chem. A* **2000**, *104*, 5625. (b) Esbou, M.; Nsangou, M.; Jaidane, N.; Lakhdar, Z. B. *Chem. Phys.* **2005**, *311*, 277.
- Matsuda, Y.; Ebata, T.; Mikami, N. *J. Chem. Phys.* **1999**, *110*, 8397.
- Wang, J.; Boyd, R. J. *J. Phys. Chem.* **1996**, *100*, 16141.
- (a) Müller, A.; Talbot, F.; Leutwyler, S. *J. Chem. Phys.* **2000**, *112*, 3717. (b) Müller, A.; Talbot, F.; Leutwyler, S. *J. Chem. Phys.* **2001**, *115*, 5192. (c) Müller, A.; Talbot, F.; Leutwyler, S. *J. Am. Chem. Soc.* **2002**, *124*, 14486.
- Chou, P. T.; Wei, C. Y. *J. Phys. Chem. B* **1997**, *101*, 9119.
- Alkorta, I.; Elguero, J. *J. Org. Chem.* **2002**, *67*, 1515.
- Müller, A.; Losada, M.; Leutwyler, S. *J. Phys. Chem. A* **2004**, *108*, 157.
- Biegler-König, F. *AIM2000*; University of Applied Sciences: Bielefeld, Germany.
- Reed, A. E.; Curtiss, L. A.; Weinhold, F. *Chem. Rev.* **1988**, *88*, 899.
- Frisch, M. J.; Trucks, G. W.; Schlegel, H. B.; Scuseria, G. E.; Robb, M. A.; Cheeseman, J. R.; Montgomery, J. A., Jr.; Vreven, T.; Kudin, K.

- N.; Burant, J. C.; Millam, J. M.; Iyengar, S. S.; Tomasi, J.; Barone, V.; Mennucci, B.; Cossi, M.; Scalmani, G.; Rega, N.; Petersson, G. A.; Nakatsuji, H.; Hada, M.; Ehara, M.; Toyota, K.; Fukuda, R.; Hasegawa, J.; Ishida, M.; Nakajima, T.; Honda, Y.; Kitao, O.; Nakai, H.; Klene, M.; Li, X.; Knox, J. E.; Hratchian, H. P.; Cross, J. B.; Adamo, C.; Jaramillo, J.; Gomperts, R.; Stratmann, R. E.; Yazyev, O.; Austin, A. J.; Cammi, R.; Pomelli, C.; Ochterski, J. W.; Ayala, P. Y.; Morokuma, K.; Voth, G. A.; Salvador, P.; Dannenberg, J. J.; Zakrzewski, V. G.; Dapprich, S.; Daniels, A. D.; Strain, M. C.; Farkas, O.; Malick, D. K.; Rabuck, A. D.; Raghavachari, K.; Foresman, J. B.; Ortiz, J. V.; Cui, Q.; Baboul, A. G.; Clifford, S.; Cioslowski, J.; Stefanov, B. B.; Liu, G.; Liashenko, A.; Piskorz, P.; Komaromi, I.; Martin, R. L.; Fox, D. J.; Keith, T.; Al-Laham, M. A.; Peng, C. Y.; Nanayakkara, A.; Challacombe, M.; Gill, P. M. W.; Johnson, B.; Chen, W.; Wong, M. W.; Gonzalez, C.; Pople, J. A. *GAUSSIAN 03*, revision B.04; Gaussian, Inc.: Pittsburgh, PA, 2003.
- (34) Held, A.; Pratt, D. W. *J. Chem. Phys.* **1992**, *96*, 4869.
- (35) Liu, Y.; Liu, W. Q.; Yang, Y.; Liu, J. Q. *Int. J. Quantum Chem.* **2006**, *106*, 2122.
- (36) Alabugin, I. V.; Manoharan, M.; Peabody, S.; Weinhold, F. *J. Am. Chem. Soc.* **2003**, *125*, 5973.
- (37) Mrázková, E.; Hobza, P. *J. Phys. Chem. A* **2003**, *107*, 1032.